

1
2 **A Unified Framework for Extreme Sub-daily Precipitation Frequency Analyses**
3 **based on Ordinary Events**
4

5 **Francesco Marra^{1,2}, Marco Borga³, Efrat Morin¹**

6 ¹The Fredy & Nadine Herrmann Institute of Earth Sciences, the Hebrew University of Jerusalem,
7 Israel.

8 ²Institute of Atmospheric Sciences and Climate, National Research Council of Italy, Bologna,
9 Italy.

10 ³Department of Land Agriculture Environment and Forestry, University of Padua, Italy.

11
12 Corresponding author: Francesco Marra (marra.francesco@mail.huji.ac.il, f.marra@isac.cnr.it)
13

14 **Key Points:**

- 15
- 16 • Unified methodology for metastatistical extreme value analysis of sub-daily precipitation across durations
 - 17 • The simplified formulation of the method permits to analyze extremes emerging from tail of ordinary events rather than entire distribution
 - 18 • Consistent definition across durations yields ordinary events which scale with the same
 - 19 scaling exponent of annual maxima
 - 20
 - 21

Abstract

23 The metastatistical extreme value approach proved promising in the frequency analysis of
24 daily precipitation from ordinary events, outperforming traditional methods based on sampled
25 extremes. However, sub-daily applications are currently restrained as it is not known if ordinary
26 events can be consistently examined over durations, and it is not clear to what extent their entire
27 distributions represent extremes. We propose here a unified definition of ordinary events across
28 durations, and suggest the simplified metastatistical extreme value formulation for dealing with
29 extremes emerging from the tail, rather than the entire distributions, of ordinary events. This
30 unified framework provides robust estimates of extreme quantiles (<10% error on the 100-year
31 from a 26-year long record), and allows scaling representations in which ordinary and extreme
32 events share the scaling exponent. Future applications could improve our knowledge of sub-daily
33 extreme precipitation and help investigating the impact of local factors and climatic forcing on
34 their frequency.

35

Plain Language Summary

37 We propose here a unified methodology to quantify the intensity of extreme rainfall of
38 short duration, such as events expected to occur on average once every 100 years. As opposed to
39 alternative methods in literature, we rely on the simultaneous analysis of all every-day rainfall
40 events, which, being much larger in number than extremes, were shown to provide improved
41 estimates for daily rainfall. We show that, under our approach, the hypothesis of every-day and
42 extreme events being similar enough holds also for short-duration rainfall. Application of our
43 method to 26 years of data from an individual station reproduces analyses based on more than
44 150 years of observations from multiple nearby stations, with less than 10% error on the
45 estimation of rain intensities expected to occur on average once every 100 years, which are not
46 directly quantifiable from the 26 years of observations. The proposed methodology could help
47 improving our knowledge of short-duration rainfall extremes, with implications for water
48 resources and risk management, and could help investigating the impact of climate change on
49 extreme rainfall events.

50

51 **1 Introduction**

52 The Metastatistical Extreme Value (MEV) framework was recently proposed for the
 53 frequency analyses of extremes under pre-asymptotic conditions. The method relies on the
 54 hypothesis that the extremes of the variable of interest emerge from the yearly distributions of
 55 underlying ordinary events, which are sampled a finite number of times every year (Marani and
 56 Ignaccolo, 2015). Once the cumulative distributions of the ordinary events $F(x, \boldsymbol{\theta}_j)$, where $\boldsymbol{\theta}_j$
 57 are the distribution parameters, are known for every year $j = 1 \dots M$, the extreme values
 58 cumulative distribution can be written as: $\zeta(x) = \frac{1}{M} \sum_{j=1}^M F_i(x, \boldsymbol{\theta}_j)^{n_j}$, where n_j is the number of
 59 ordinary events observed in the j -th year (Zorzetto et al., 2016). The framework can include any
 60 class of distributions for F , and allows to consider multiple types of ordinary events (e.g., non-
 61 tropical and tropical cyclones) to derive compound extreme value distributions (Marra et al.,
 62 2019; Miniussi et al., 2020). Making use of the full available data record, MEV also largely
 63 decreases the parameter estimation uncertainty and the stochastic uncertainty related to the
 64 sampling of extremes.

65 It can be shown that when the inter-annual variability of the ordinary events can be
 66 neglected (i.e., $\boldsymbol{\theta}_j \approx \boldsymbol{\theta}_k, \forall j, k$) and the focus is on extreme quantiles (i.e., $F \rightarrow 1$), the inter-
 67 annual variability of the number of yearly events also becomes negligible. In these conditions, a
 68 simplified MEV formulation (SMEV), closely resembling ordinary statistics, can be written:
 69 $\zeta(x) \approx F(x, \boldsymbol{\theta})^n$, where n is here the average number of ordinary events per year (Marra et al.,
 70 2019). SMEV was originally proposed as an instantaneous limit ($M \rightarrow 0$) of MEV for the
 71 analysis of nonstationary processes. However, when tested for extreme value analyses on
 72 observational records, SMEV was found to perform similarly, even if less accurately than MEV,
 73 and to be preferable when the small number of ordinary events per year prevents to accurately
 74 estimate parameters for individual years ($n \lesssim 20$) (Schellander et al., 2019; Miniussi and
 75 Marani, 2020). Owing to the largely increased data sample used to estimate the distribution
 76 parameters (all years are used together), SMEV permits to focus on the tail of the ordinary events
 77 distribution by left-censoring the data (Marra et al., 2019). It should be noted that this is not
 78 equivalent to threshold exceedance methods as, in such cases, the information below threshold is
 79 discarded and results hold only asymptotically for thresholds tending to the upper limit of the

80 distribution support (Davison and Smith, 1990), while SMEV describes tails which include large
81 portions of the data and whose definition accounts for the whole data sample.

82 So far, MEV methods have been mostly used for the analysis of extreme daily
83 precipitation relying on Weibull distributions to describe the ordinary events (e.g., Marani and
84 Ignaccolo, 2015; Zorzetto et al., 2016; Miniussi and Marani, 2020). Results showed a number of
85 advantages over traditional methods based on the sampled extremes: (i) rare quantiles,
86 corresponding to return periods longer than the available data record, are estimated with
87 significantly reduced errors; (ii) short records are sufficient to obtain robust estimates; (iii) the
88 method is less sensitive to measurement errors typically affecting extremes (Zorzetto et al., 2016;
89 Marra et al., 2018; Schellander et al., 2019; Miniussi and Marani, 2020; Zorzetto and Marani,
90 2020). Extending the applicability of MEV to sub-daily durations by means of a unified
91 methodology that allows to examine ordinary events across durations could pose the bases for
92 more general frameworks relying on the scaling properties of ordinary events. This could
93 improve our understanding of extreme precipitation at the global scale and provide more
94 accurate information for hydraulic infrastructure design and risk management.

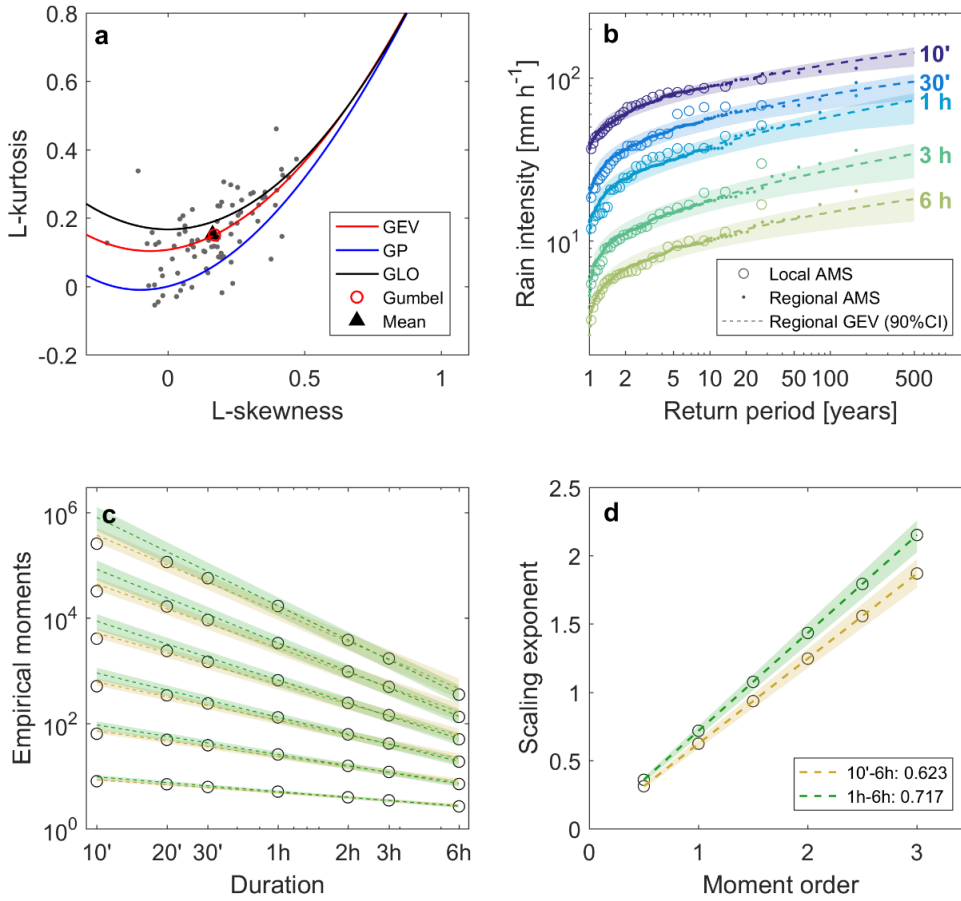
95 Two knowledge gaps currently restrain the application of MEV to sub-daily durations.
96 First, the only method so far proposed to define sub-daily ordinary events is based on the
97 temporal autocorrelation of the individual time series and do not permit to consider multiple
98 durations together (Marra et al., 2018). Second, the results reported above only pertain to
99 extremes emerging from the entire yearly distributions of ordinary events. This assumption is in
100 contrast with results showing that sub-daily precipitation is better described by more general
101 distributions, whose tails only can be approximated by stretched-exponential (e.g., Weibull) or
102 power-type distributions (e.g., Papalexiou et al., 2018; Papalexiou, 2018). Here, we address these
103 gaps by (a) proposing a consistent definition of ordinary events which allows scaling
104 representations across durations, and (b) suggesting SMEV as a viable option for dealing with
105 extremes emerging from the tail of the ordinary events distribution, as opposed to their entire
106 distributions. We evaluate the robustness of the proposed MEV and SMEV approaches on a
107 study case in the southeastern Mediterranean coast for which 26 years of 10-min data are
108 available. We rely on regional estimates of rare quantiles from 9 stations (>150 years of record in
109 total) as a reference.

110 2 Methods

111 We propose to define ordinary events based on *storms*, i.e. consecutive wet events
112 separated by dry hiatuses whose length is to be determined based on the climatology of the region.
113 Ordinary events can then be computed as the maxima intensities observed within each storm using
114 moving windows of the desired duration. In this way, ordinary events are directly related to
115 meteorological features, and their number remains consistent across durations.

116 Series of 10-min precipitation data are collected for 9 quality-checked automatic stations
117 (164-year record in total) in the south-eastern Mediterranean coast. Distance between the stations
118 ranges between 1.5 and 70 km (27 ± 16 km) and individual records span 10 to 26 years ($18.2 \pm$
119 6.1 years). Homogeneity of the region was ensured using the method based on the coefficient of
120 L-variation recommended by Hosking and Wallis (1997) ($H < 0.25$ for all durations), so that the
121 stations could be collectively used in a regional framework to estimate extremely low yearly
122 exceedance probabilities. Reference quantiles are computed from the 9 stations using the regional
123 L-moments method by Hosking and Wallis (1997) and the generalized extreme value (GEV)
124 distribution (Fig. 1) by normalizing the annual maxima over their mean values.

125



126

127 **Figure 1.** Regional analysis and scaling of the annual maxima. (a) L-Moments ratio diagram for all the
 128 stations and durations, the theoretical moments for generalized extreme value (GEV), generalized Pareto
 129 (GP) and generalized logistic (GLO) distributions are shown. (b) Regional GEV distributions (dashed
 130 lines) estimated using the regional L-moments framework by Hosking and Wallis (1997); shaded areas
 131 show the 90% confidence interval obtained via bootstrap with replacement among the regional annual
 132 maxima (AMS); circles show the AMS observed at Zykhron Yaaqov station (frequency is estimated using
 133 the Weibull plotting positions), while dots show the AMS from all the 9 stations rescaled to the Zykhron
 134 Yaaqov mean. (c) Raw moments of the AMS. Colored lines show the regressions obtained using the full
 135 temporal domain (10 min – 6 hours; orange, shaded area represent the 90% confidence interval from 10³
 136 bootstrap samples with replacement among the years) and the 1 h – 6 h interval (green); (d) Scaling
 137 exponent of the AMS obtained using the full temporal domain (10 min – 6 hours; orange) and the 1 h – 6
 138 h interval (green).

139

140 Following previous studies in similar climates, we require at least six-dry-hour hiatuses
 141 (i.e., lower than the minimum rain amount reported in the data, 0.1 mm, over all 10-min intervals

142 for 6 consecutive hours) to separate storms (Restrepo-Posada and Eagleson, 1982; Tarolli et al.,
 143 2012), but general applications should use a definition based on the local climatology. Storms
 144 lasting less than 30 min (three time intervals, in our case) are removed. We focus on durations
 145 between 10-min and 6-hour (10-min, 20-min, 30-min, 1-hour, 3-hour, 6-hour), a choice driven by
 146 the temporal resolution of the data (10-min) and the dry hiatus used to separate storms (6-hour).

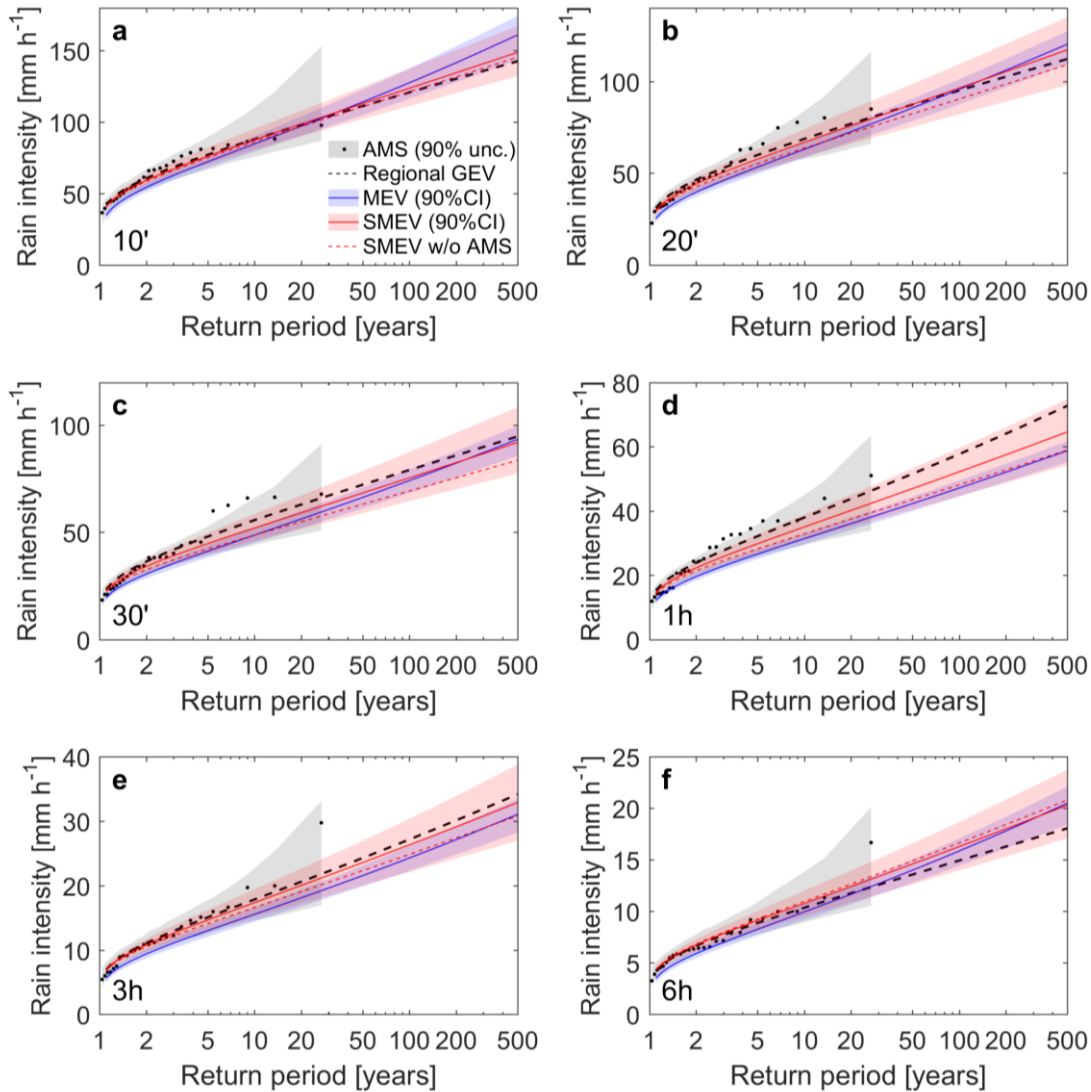
147 MEV and SMEV are here applied *at-site* focusing on the longest recording station (Zikhron
 148 Yaaqov, 26-year). Complying with previous MEV applications, ordinary events are described
 149 using Weibull distributions in the form $F(x; \lambda, \kappa) = 1 - e^{-\left(\frac{x}{\lambda}\right)^\kappa}$, where λ and κ are the scale and
 150 shape parameters, respectively (Zorzetto et al., 2016). Such a model was shown as appropriate for
 151 the here-examined region (Marra et al., 2019). Three MEV parameters are obtained for every year:
 152 λ_j and κ_j are estimated from all the yearly ordinary events by using the method of the L-moments
 153 (Hosking, 1990), and n_j as the number of ordinary events in the j -th year. Extreme quantiles are
 154 then computed by numerically inverting the MEV cumulative distribution function (Zorzetto et
 155 al., 2016; Marra et al., 2018).

156 Neglecting inter-annual variability, SMEV only requires three parameters: λ and κ are
 157 estimated left-censoring the low portion of the ordinary events and using a least-squares regression
 158 in Weibull-transformed coordinates on the remaining data points (Marani and Ignaccolo, 2015),
 159 while n is the mean number of ordinary events per year ($n = \frac{\sum n_j}{M}$). It is worth noting that, when
 160 based on Weibull, the SMEV distribution becomes an exponentiated Weibull distribution
 161 (Nadarajah et al., 2013). Following previous results for the region, the ordinary events tail is here
 162 defined as the largest 25% of the ordinary events (Marra et al., 2019). It should be however noted
 163 that the definition of the tails is case-dependent and should be selected using sensitivity analyses
 164 (as in Marra et al., 2019); for example, definition of the tail as the largest 45%-20% of the ordinary
 165 events was found appropriate for the study region. Extreme quantiles are computed inverting the
 166 SMEV cumulative distribution function. In addition, in order to better evaluate the robustness of
 167 SMEV to represent the distribution of out-of-sample extremes, a second set of parameters and
 168 quantiles is derived by also censoring all the annual maxima, so to obtain results fully independent
 169 from the observed annual maxima. For all methods, confidence intervals in parameters and
 170 quantiles are computed via bootstrap with replacement (10^3 repetitions) among the years in the
 171 record (Overeem et al., 2008).

172 **3 Results and discussion**

173 Application of MEV and SMEV to the here defined sub-daily ordinary events provides
174 robust estimates of extreme quantiles (Fig. 2), with the estimated MEV (blue solid line and 90%
175 confidence interval) and SMEV (red) distributions being generally consistent with the regional
176 reference, and only MEV slightly underestimating quantiles for 1- and 3-hour durations (the
177 reference lies outside of the 90% confidence interval). Thanks to the focus on the ordinary events
178 tail, SMEV provides more accurate estimates (<10% error on the 100-year quantiles for all
179 durations, <12.5% for 500-year) than MEV (<20%) but, due to the smaller data sample used to
180 estimate the parameters, is characterized by larger uncertainty. Quantiles obtained independently
181 from the observed annual maxima (red dashed lines) lie within the confidence interval of SMEV,
182 and never exceed 20% error, even for 500-year return levels. Similarly, the observed annual
183 maxima (black dots, plotted using the Weibull plotting positions) lie within the area in which we
184 expect to see 90% of the annual maxima *if* they were actually sampled from SMEV (shaded in
185 grey, obtained from 10^3 random sampling from SMEV). These observations support the
186 robustness of the SMEV approach.

187



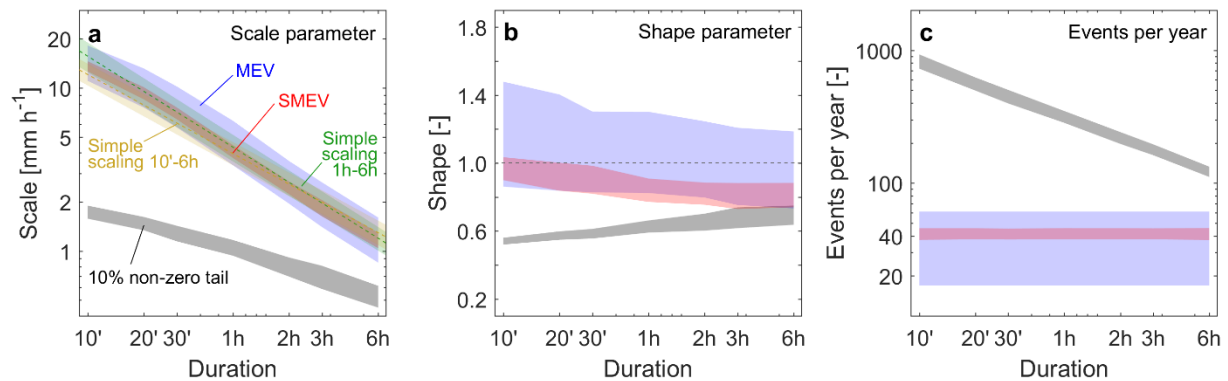
188

189 **Figure 2.** Quantiles estimated using MEV (blue solid line), SMEV (red solid line) for 10-min to 6-hour
 190 durations (a-f); blue and red shaded areas show the corresponding 90% confidence intervals (10^3
 191 bootstrap samples with replacement among the years). Black dots show the observed annual maxima
 192 (AMS) and dashed black line the regional GEV estimate obtained from 9 stations in the region
 193 (reference). Shaded in grey are the areas in which 90% of the annual maxima are expected to lie *if*
 194 were sampled from SMEV. Red dashed lines represent quantiles obtained using SMEV and censoring the
 195 annual maxima.

196

197 The scaling of MEV and SMEV parameters with duration is presented in Fig. 3, noting
 198 that blue shaded area represents the 90% inter-annual variability of MEV parameters, and red
 199 and grey areas represent the 90% confidence intervals (bootstrap among the years) of SMEV and

200 non-zero-tail parameters, respectively. It is interesting to see a decrease of the shape parameter
 201 with increasing duration (Fig. 3b). This translates into heavier tails of the distribution of ordinary
 202 events at longer durations and, due to the consistent definition of ordinary events, of the resulting
 203 extreme value distribution. Despite seemingly contradicting previous results in which the tail of
 204 non-zero time intervals was examined (e.g., Papalexiou et al., 2018, shown here in grey), this is
 205 explained by the dramatic change in the number of non-zero time intervals per year (Fig. 3c).
 206 Using a consistent definition of the ordinary events in which their number is the same across
 207 durations, MEV and SMEV scale parameters scale with duration with the same scaling exponent
 208 of the annual maxima above 1-hour (Fig. 3a and Fig. 1). Notably, this is the temporal domain in
 209 which the simple scaling behavior of annual maxima is generally considered more robust
 210 (Burlando and Rosso, 1996; Ceresetti et al., 2010). This property suggests that extremes are
 211 indeed samples from the tail of the ordinary events, and opens MEV methods to applications in
 212 which multiple durations are used simultaneously (e.g., Burlando and Rosso, 1996; Langousis
 213 and Veneziano, 2007; Innocenti et al., 2017; Emmanouil et al., 2020). Overall, the use of
 214 consistent ordinary events across durations permits to examine the scaling behavior in all rain
 215 events, including different (if any) scaling behaviors between extreme and ordinary events.
 216



217

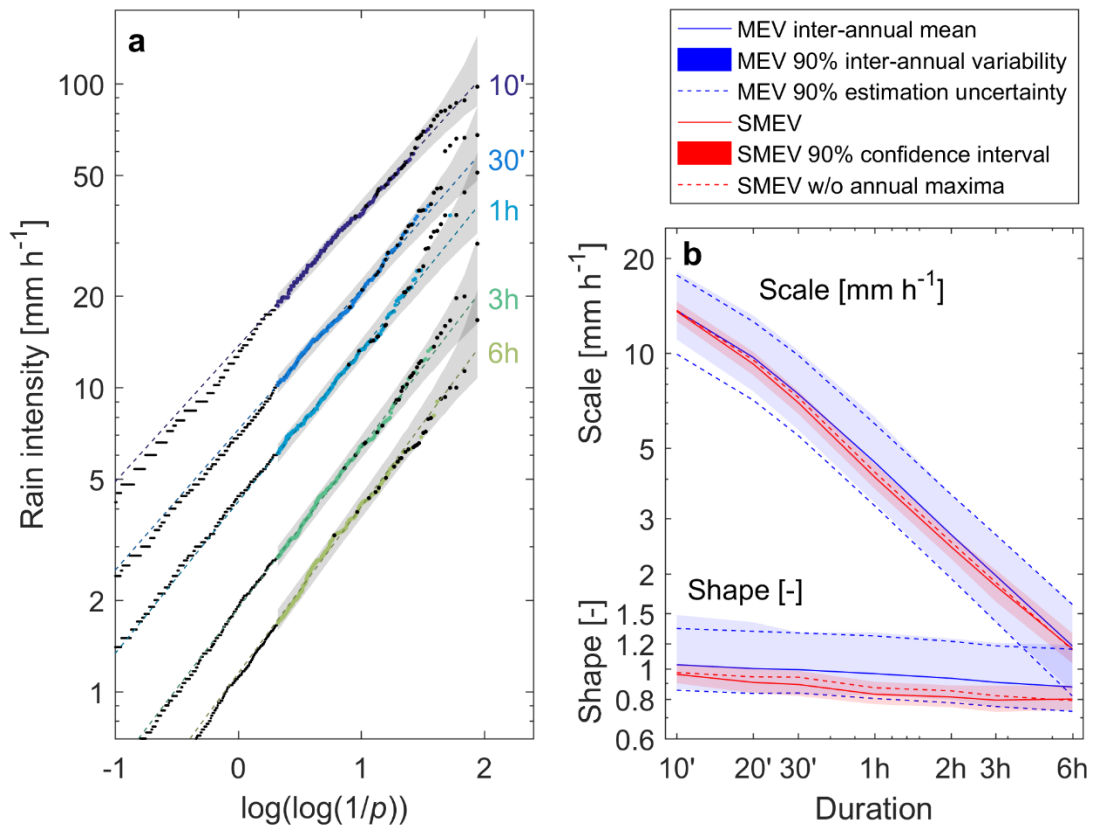
218 **Figure 3.** Scaling of MEV and SMEV parameters with duration; blue shaded area represents the 90%
 219 inter-annual variability of MEV parameters, and red and grey areas represent the 90% confidence
 220 intervals (bootstrap among the years) of SMEV and 10% non-zero tail (as in Papalexiou et al., 2018)
 221 parameters, respectively. (a) Scaling of the scale parameters with duration for MEV (blue), SMEV (red)
 222 and 10% non-zero tail (grey). Simple scaling relations from annual maxima are superimposed (10 min–6
 223 h in orange, 1 h–6 h in in green, see Fig. 1); within the uncertainties, MEV and SMEV scale parameters
 224 share the scaling exponent with annual maxima, especially the 1 h–6 h (green); (b) Scaling of the shape

225 parameters with duration. The shape parameter of the non-zero tail increases with duration as reported by
226 other studies (e.g., Papalexiou et al., 2018), while an opposite behavior is reported for the MEV and
227 SMEV; for the case of SMEV, the decrease is larger than the parameter estimation uncertainty; (c)
228 Scaling of the number of ordinary events per year with duration. The proposed definition makes their
229 number independent on duration (~40 events per year in this case). The marked decrease of the number of
230 non-zero time intervals (grey) explains the different behaviors observed for the shape parameters between
231 non-zero tail and MEV methods.

232

233 We conclude showing further evidence for the emergence of extreme sub-daily
234 precipitation from the tail of ordinary events. In the examined case (Fig. 4a, which confirms what
235 observed in Fig. 2), the whole tail of ordinary events (colored dots), including annual maxima
236 (thick black dots), are likely samples from a unique Weibull distribution whose parameters are
237 here estimated explicitly censoring the observed annual maxima values (dashed lines, shaded
238 areas represent 90% sampling uncertainty under the local climatology; note that 10% of the
239 points are expected to lie outside of this area). Additionally, the robustness of SMEV in
240 extracting information from ordinary events emerges in that the parameters estimated censoring
241 the annual maxima (red dashed lines in Fig. 4b) are indistinguishable (i.e. within the red-shaded
242 confidence interval) from the ones describing the whole tail (red solid line). Despite relying on
243 an average of more than 40 ordinary events per year, the here analyzed data did not allow to
244 separate the inter-annual variability of MEV parameters (shaded blue area in Fig. 4b) from the
245 yearly parameter estimation uncertainty (blue dashed lines).

246



247
 248 **Figure 4.** Robustness of MEV and SMEV assumptions. (a) Weibull plot (on the x-axis, p is the
 249 exceedance probability, i.e., $1 - F$, in our notation) showing the ordinary events for the examined
 250 durations (dots, the 25% tail used in SMEV is colored according to the duration and annual maxima are in
 251 thick black), Weibull distributions (dashed lines) whose parameters are estimated fitting the 25% tail and
 252 explicitly censoring the observed annual maxima values (thick black dots), and sampling uncertainty from
 253 the Weibull distribution (90% interval from $2 \cdot 10^3$ random samples); (b) Weibull parameters estimated
 254 using MEV and SMEV. Inter-annual variability of MEV parameters (blue shaded area) almost perfectly
 255 overlaps with parameter estimation uncertainty (blue dashed lines; 10^3 random samples from a Weibull
 256 distribution described by the mean MEV parameters). SMEV parameters computed censoring the annual
 257 maxima (red dashed lines) are within the 90% confidence interval of the SMEV parameters (10^3 bootstrap
 258 repetitions with replacement among the years).

259

260 4 Closing statement

261 We proposed a consistent definition of ordinary events based on independent storms to
 262 use the Metastatistical Extreme Value (MEV) framework across durations, and suggested the

263 simplified MEV formulation (SMEV) as an option to deal with extremes emerging from the tail
264 of the ordinary events rather than their entire distribution. This definition of ordinary events
265 allowed to effectively use MEV methods for sub-daily extreme precipitation frequency analyses,
266 and permitted a scaling representation in which ordinary events scale with the same exponent of
267 the observed annual maxima. Owing to its focus on the tail of the ordinary events distribution,
268 SMEV provided estimates of 100-year quantiles with less than 10% error (12.5% for the 500-
269 year event) from only 26 years of data (up to ~20% for MEV). These results support the use of
270 MEV methods for sub-daily (and sub-hourly) precipitation frequency analyses, and open to the
271 use of analytical frameworks exploiting these methods across durations. Applications of the
272 approach could improve our knowledge of extreme sub-daily precipitation at the global scale
273 with important implications for hydraulic design and risk management. Additionally, the analysis
274 of SMEV parameters could help investigating local properties of extreme precipitation that are
275 generally masked by the stochastic uncertainties characterizing the sampling of extremes, such as
276 their response to local and climate forcing.

277 **Acknowledgments**

278 The authors declare no conflict of interest. Precipitation data was provided by the Israel
279 Meteorological Service and can be retrieved from www.ims.gov.il. Codes and data produced in
280 the study are available at doi:10.5281/zenodo.3902761. The study was funded by the Israel
281 Science Foundation [grant no. 1069/18], the Israel Ministry of Science and Technology [grant
282 no. 61792], and by KKL [grant no. 30-7-010-11]. This is a contribution to the HyMeX program.
283 Authors contribution: Conceptualization: FM, MB; Funding acquisition: EM, FM; Formal
284 analyses, Data curation, Paper writing: FM; Paper review and editing: all authors.

285 **References**

- 286 Burlando, P., & Rosso, R. (1996), Scaling and multiscaling models of depth-duration-frequency
287 curves for storm precipitation. *Journal of Hydrology*, 187, 45-64. Doi:10.1016/S0022-
288 1694(96)03086-7
- 289 Ceresetti, D., Molinié, G., & Creutin, J.-D. (2010), Scaling properties of heavy rainfall at short
290 duration: A regional analysis, *Water Resources Research*, 46, W09531,
291 doi:10.1029/2009WR008603

- 292 Davison, A. C., & Smith, R. L. (1990), Models for exceedances over high thresholds. *Journal of*
293 *the Royal Statistical Society, Series B (Methodological)*, 52(3), 393-442, doi:10.1111/j.2517-
294 6161.1990.tb01796.x
- 295 Emmanouil, S., Langousis, A., Nikolopoulos, & E. I., Anagnostou, E. N. (2020), Quantitative
296 assessment of annual maxima, peaks-over-threshold and multifractal parametric approaches
297 in estimating intensity-duration-frequency curves from short rainfall records. *Journal of*
298 *Hydrology*, doi:10.1016/j.jhydrol.2020.125151
- 299 Hosking, J. R. M. (1990), L-moments: analysis and estimation of distributions using linear
300 combinations of order statistics. *Journal of the Royal Statistical Society, Series B*
301 *(Methodological)*, 52(1), 105–124.
- 302 Hosking, J. R. M., & Wallis, J. R. (1997), Regional Frequency Analysis: An Approach Based on
303 l-moments. *Cambridge University Press, UK*. doi:10.1017/cbo9780511529443
- 304 Innocenti, S., Mailhot, A., & Frigon, A. (2017), Simple scaling of extreme precipitation in North
305 America, *Hydrology and Earth System Science*, 21, 5823–5846, doi:10.5194/hess-21-5823-
306 2017
- 307 Langousis, A., & Veneziano, D. (2007), Intensity-duration-frequency curves from scaling
308 representations of rainfall, *Water Resources Research*, 43, W02422,
309 doi:10.1029/2006WR005245
- 310 Marani, M., & Ignaccolo, M. (2015), A metastatistical approach to rainfall extremes. *Advances*
311 *in Water Resources*, 79, 121–126. doi:10.1016/j.advwatres.2015.03.001
- 312 Marra, F., Nikolopoulos, E. I., Anagnostou, E. N., & Morin, E. (2018), Metastatistical extreme
313 value analysis of hourly rainfall from short records: Estimation of high quantiles and impact
314 of measurement errors. *Advances in Water Resources*, 117, 27–39,
315 doi:10.1016/j.advwatres.2018.05.001
- 316 Marra, F., Zocatelli, D., Armon, M., & Morin, E. (2019), A simplified MEV formulation to
317 model extremes emerging from multiple nonstationary underlying processes. *Advances in*
318 *Water Resources*, 127, 280-290, doi:10.1016/j.advwatres.2019.04.002
- 319 Miniussi, A., & Marani, M. (2020), Estimation of daily rainfall extremes through the
320 Metastatistical Extreme Value Distribution: uncertainty minimization and implications for
321 trend detection. *Water Resources Research*, e2019WR026535, doi:10.1029/2019WR026535

- 322 Miniussi, A., Villarini, G., & Marani, M. (2020), Analyses through the metastatistical extreme
323 value distribution identify contributions of tropical cyclones to rainfall extremes in the
324 eastern United States. *Geophysical Research Letters*, *47*, e2020GL087238,
325 doi:10.1029/2020GL087238
- 326 Nadarajah, S., Cordeiro, G. M., & Ortega, E. M. M. (2013), The exponentiated Weibull
327 distribution: a survey. *Statistical Papers*, *54*, 839-877, doi:10.1007/s00362-012-0466-x
- 328 Overeem, A., Buishand, A., & Holleman, I. (2008), Rainfall depth-duration-frequency curves
329 and their uncertainties. *Journal of Hydrology*, *348*, 124–134,
330 doi:10.1016/j.jhydrol.2007.09.044
- 331 Papalexiou, S. M. (2018). Unified theory for stochastic modelling of hydroclimatic processes:
332 Preserving marginal distributions, correlation structures, and intermittency. *Advances in*
333 *Water Resources*, *115*, 234-252, doi:10.1016/j.advwatres.2018.02.013
- 334 Papalexiou, S. M., AghaKouchak, A., & Foufoula-Georgiou, E. (2018), A diagnostic framework
335 for understanding climatology of tails of hourly precipitation extremes in the United States.
336 *Water Resources Research*, *54*, doi:10.1029/2018WR022732
- 337 Restrepo-Posada, P. J., & Eagleson, P. S. (1982), Identification of independent rainstorms,
338 *Journal of Hydrology*, *55*, 303–319, doi:10.1016/0022-1694(82)90136-6
- 339 Schellander, H., Lieb, A., & Hell, T. (2019), Error structure of Metastatistical and Generalized
340 Extreme Value Distributions for modeling extreme rainfall in Austria. *Earth and Space*
341 *Science*, *6*(9), 1616–1632, doi:10.1029/2019EA000557
- 342 Tarolli, P., Borga, M., Morin, E., & Delrieu, G. (2012), Analysis of flash flood regimes in the
343 North-Western and South-Eastern Mediterranean regions, *Natural Hazards and Earth System*
344 *Sciences*, *12*, 1255–1265, doi:10.5194/nhess-12-1255-2012
- 345 Zorzetto, E., Botter, G., & Marani, M. (2016), On the emergence of rainfall extremes from
346 ordinary events. *Geophysical Research Letters*, *43*, 8076–8082, doi:10.1002/2016GL069445
- 347 Zorzetto, E., & Marani, M. (2020), Extreme value metastatistical analysis of remotely sensed
348 rainfall in ungauged areas: spatial downscaling and error modeling. *Advances in Water*
349 *Resources*, *135*, 103483, doi:10.1016/j.advwatres.2019.103483